Alkyl and Aryl Substituted Corroles. 1. Synthesis and Characterization of Free Base and Cobalt Containing Derivatives. X-ray Structure of $(Me_4Ph_5Cor)Co(py)_2$

Roger Guilard,*,† Claude P. Gros,† Frédéric Bolze,† François Jérôme,† Zhongping Ou,‡ Jianguo Shao,‡ Jean Fischer,§ Raymond Weiss,§ and Karl M. Kadish*,‡

LIMSAG UMR 5633, Faculté des Sciences Gabriel, Université de Bourgogne, 6, Boulevard Gabriel, 21000 Dijon, France, Department of Chemistry, University of Houston, Houston, Texas 77204-5641, and Institut Le Bel, Université Louis Pasteur, 4 Rue Blaise Pascal, 67000 Strasbourg, France

Received February 9, 2001

The synthesis, spectroscopic properties, and electrochemistry of six different alkyl- and aryl-substituted Co(III) corroles are presented. The investigated compounds contain methyl, ethyl, phenyl, or substituted phenyl groups at the eight β-positions of the corrole macrocycle and four derivatives also contain a phenyl group at the 10-*meso* position of the macrocycle. Each cobalt corrole undergoes four reversible oxidations in CH_2Cl_2 containing 0.1 M tetra-*n*-butylammonium perchlorate and exists as a dimer in its singly and doubly oxidized forms. The difference in potential between the first two oxidations is associated with the degree of interaction between the two corrole units of the dimer and ranges from an upper value of 0.62 V, in the case of $(Me_6Et_2Cor)Co$, to a lower value of about 0.17 V, in the case of four compounds which have a phenyl group located at the 10-*meso* position of the macrocycle. These Co(III) corroles strongly coordinate two pyridine molecules or one carbon monoxide molecule in CH_2Cl_2 media, and ligand binding constants were evaluated using spectroscopic and electrochemical methods. The structure of $(Me_4Ph_5Cor)Co(py)_2$ was also determined by X-ray diffraction. Crystal data: $(Me_4Ph_5Cor)Co(py)_2 \cdot 3CH_2Cl_2 \cdot H_2O$, orthorhombic, $a = 19.5690(4)$ Å, $b = 17.1070(6)$ Å, $c = 15.9160(6)$ Å, $V = 5328.2(5)$ Å^3, space group $Pna2_1$, $Z = 2$, 35 460 observations, $R(F) = 0.069$.

Introduction

A number of different corroles and metallocorroles have now been synthesized. These include the well-known octaethyl- and octamethylcorroles as well as several derivatives with mixed ethyl and methyl substituents at the eight β-pyrrole positions of the macrocycle.[1,2] Corroles containing *meso*-substituted C_6H_5, C_6F_5, or C_6H_4X groups where X is an electron-donating or electron-withdrawing substituent are also known.[3−6]

The 5- or 10-phenyl substituted corroles with alkyl substituents in the β-pyrrole positions often exhibit a reduced stability in solution; these compounds undergo an oxidative ring opening when left in solution in the presence of air and light and are converted to the corresponding biliverdin among other decomposition products.[6] However, the introduction of aryl groups at the 2, 3, 17, and 18 β-pyrrole positions of the corrole macrocycle helps to prevent oxidative attack of the ring which would result in cleavage of the 1,19-direct pyrrole−pyrrole bond.[6−8] Interestingly, and in contrast to what is observed in porphyrin systems, steric crowding about the periphery of a corrole macrocycle does not prevent the corrole from retaining a planar conformation as was demonstrated in the case of a cobalt(III) *meso*-phenyl substituted complex.[9]

A recent electrochemical study of $(Et_8Cor)M$ where M = Co, Cu, or Ni showed the formation of singly and doubly oxidized dimers upon the abstraction of one or two electrons in CH_2Cl_2 and other noncoordinating media.[10] The interaction between the two corrole units in the oxidized $(Et_8Cor)M$ complexes will depend on the specific metal ion and its oxidation state as well as upon the degree of coordination of the metal ion. It should also depend on the specific substituents on the corrole macrocycle, but no report of dimer formation from monomeric metallocorroles has ever appeared for complexes other than those having an $(Et_8Cor)M$ structure. Thus, to examine the influence of peripheral crowding on the chemistry, electrochemistry, and dimerization of other related corroles, we have synthesized a series of derivatives with phenyl and anisyl substituents at the 2, 3, 10, 17, and 18 β-pyrrole positions of the corrole macrocycle. These compounds, which are described in the present paper, are shown in Chart 1. This paper also reports the ligand binding properties of each cobalt corrole in

† Université de Bourgogne.
‡ University of Houston.
§ Université Louis Pasteur.

(1) Paolesse, R. In *The Porphyrin Handbook*; Kadish, K. M., Smith, K. M., Guilard, R., Eds.; Academic Press: San Diego, CA, 2000; Vol. 2, pp 201−232.
(2) Erben, C.; Will, S.; Kadish, K. M. In *The Porphyrin Handbook*; Kadish, K. M., Smith, K. M., Guilard, R., Eds.; Academic Press: San Diego, CA, 2000; Vol. 2, pp 233−300.
(3) Adamian, V. A.; D'Souza, F.; Licoccia, S.; Di Vona, M. L.; Tassoni, E.; Paolesse, R.; Boschi, T.; Kadish, K. M. *Inorg. Chem.* **1995**, *34*, 532−540.
(4) Gross, Z.; Simkhovich, L.; Galili, N. *Chem. Commun.* **1999**, 599−600.
(5) Simkhovich, L.; Galili, J.; Saltsman, I.; Goldberg, I.; Gross, Z. *Inorg. Chem.* **2000**, *39*, 2704−2705.
(6) Tardieux, C.; Gros, C. P.; Guilard, R. *J. Heterocycl. Chem.* **1998**, *35*, 965−970.
(7) Jérôme, F.; Gros, C. P.; Tardieux, C.; Barbe, J.-M.; Guilard, R. *Chem. Commun.* **1998**, 2007−2008.
(8) Jérôme, F.; Gros, C. P.; Tardieux, C.; Barbe, J.-M.; Guilard, R. *New J. Chem.* **1998**, *22*, 1327−1329.
(9) Paolesse, R.; Licoccia, S.; Bandoli, G.; Dolmella, A.; Boschi, T. *Inorg. Chem.* **1994**, *33*, 1171−1176.
(10) Kadish, K. M.; Adamian, V. A.; Van Caemelbecke, E.; Gueletii, E.; Will, S.; Erben, C.; Vogel, E. *J. Am. Chem. Soc.* **1998**, *120*, 11986−11993.

10.1021/ic010177+ CCC: $20.00
Published on Web 09/04/2001

Chart 1

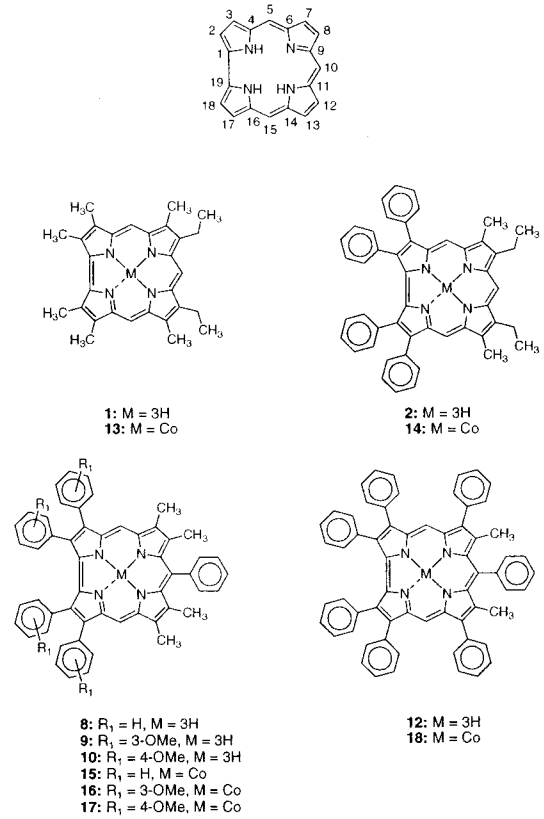

CH_2Cl_2, and these data serve as the basis for understanding the ligand binding and electrochemical reactions of related linked bis-corroles whose synthesis and properties are described in the following paper in this issue.[11] In addition, an X-ray structure of one complex, $(Me_4Ph_5Cor)Co(py)_2$, is presented.

Experimental Section

Instrumentation. ^{1}H NMR spectra were recorded on a Bruker AC 200 Fourier transform spectrometer at the Centre de Spectrométrie Moléculaire de l'Université de Bourgogne. Chemical shifts are expressed in parts per million relative to chloroform (7.258 ppm). Microanalyses were performed at the Université de Bourgogne on a Fisons EA 1108 CHNS instrument. UV−visible spectra were recorded on a Varian Cary 1 spectrophotometer or on an HP 8453 UV−visible spectrophotometer in the case of spectroelectrochemistry. Mass spectra were obtained with a Kratos Concept 32 S spectrometer in EI mode. Cyclic voltammetry was carried out with an EG&G model 173 potentiostat. A three-electrode system was used and consisted of a glassy carbon or platinum disk working electrode, a platinum wire counter electrode, and a saturated calomel electrode (SCE) as the reference electrode. The SCE was separated from the bulk of the solution by a fritted-glass bridge of low porosity which contained the solvent/supporting electrolyte mixture. All potentials are referenced to the SCE. Cyclic voltammetry under different CO partial pressures was carried out in a sealed cell. UV−vis spectroelectrochemical experiments were performed with a home-built platinum thin-layer cell of the type described in the literature.[12] Potentials were applied and monitored with an EG&G Princeton Applied Research model 173 potentiostat.

Infrared spectra were recorded on an FTIR Nicolet Magna-IR 550 spectrometer. The background was obtained by recording the IR spectrum of CH_2Cl_2 saturated by CO, and the IR spectrum of the compound under CO was obtained after bubbling CO through the solution.

Equilibrium Measurements. The binding of pyridine to each Co(III) corrole was carried out in CH_2Cl_2 and the room temperature (296 K) reaction monitored by UV−visible spectroscopy. The absorbance data were then fitted to the Hill equation:[13]

$$\log((A_i - A_0)/(A_f - A_i)) = \log K + p \log [py] \qquad (1)$$

where A_i = absorbance at a specific concentration of pyridine; A_0 = initial absorbance where [py] = 0, and A_f = final absorbance where the fully ligated corrole is the only species present. Values of log K were obtained from the intercept of the regression line in a plot of $\log((A_i - A_0)/(A_f - A_i))$ vs log [py]. The slope, p, should be equal to the number of axially coordinated ligands. The concentration of the corroles for these measurements was 5×10^{-6} M, and that of pyridine was in the range of 10^{-5} to 0.5 M.

A calibrated gas tight syringe was used to introduce CO into solutions of CH_2Cl_2. The pressure of CO within the gas tight syringe ($P_{injected}$) was read from the barometer before each injection. The volume of the titration vessel above the solution (V_{vessel}) was 175 mL. Thus, by systematically injecting into the vessel a known volume ($V_{injected}$) of CO gas, we were able to calculate the partial pressure of CO (P_{CO}) at each step in the titration as being equal to $(V_{injected}/V_{vessel})P_{injected}$. The vessel was vigorously shaken for 3 min after introducing CO to ensure equilibrium before recording each UV−visible spectrum at a given partial pressure of CO, and the Hill equation was used to analyze the data as a function of CO partial pressure. $P_{1/2}^{CO}$, the pressure of CO when the ligand binding reaction had proceeded halfway, was used to represent the formation constant. The solubility coefficient of CO in CH_2Cl_2 was taken as 6.7×10^{-3} M/atm,[14] and this value was used to calculate the formation constant, K.

Chemicals and Reagents. Basic alumina (Merck; usually Brockmann Grade III, i.e. deactivated with 6% water) was used for column chromatography. Absolute dichloromethane (CH_2Cl_2) was obtained from Fluka Chemical Co. and used as received. Tetra-*n*-butylammonium perchlorate (TBAP, Fluka Chemical Co.) was twice recrystallized from absolute ethanol and dried in a vacuum oven at 40 °C for a week prior to use.

2,3,7,13,17,18-Hexamethyl-8,12-diethylcorrole (**1**),[15−17] 7,13-dimethyl-8,12-diethyl-2,3,17,18-tetraphenylcorrole (**2**),[6] 5,5′-dicarboxy-3,3′,4,4′-tetramethyldipyrryltoluene (**3**),[16] 3,4-diethyl-2-formylpyrrole (**4**),[15] ethyl 4-methyl-3-phenyl-*1H*-pyrrole-2-carboxylate (**5**),[8] 3,4-di(*p*-anisil)pyrrole (**7b**)[7] were synthesized as described in the literature.

3,4-Di(*m*-anisyl)pyrrole-2,5-dicarboxylic Acid (6a). Sodium (14 g) was dissolved in 150 mL of absolute methanol under an atmosphere of nitrogen in a 500 mL three-necked flask equipped with a nitrogen inlet and reflux condenser. The solution was cooled to room temperature, and 12 g of dimethyl *N*-acetyliminodiacetate (0.06 mol) dissolved in 50 mL of dry methanol was added to the sodium methoxide solution while the mixture was being stirred by means of a mechanical stirrer. Solid 3,3′-dimethoxybenzyl (11 g, 0.040 mol) was then added in fractions. Stirring was continued at room temperature until all of the 3,3′-dimethoxybenzyl was dissolved. The reaction mixture was slowly heated to the boiling point, then refluxed for 4 h, and poured into 1 L of cold water after which the unreacted 3,3′-dimethoxybenzyl (yellow precipitate) was filtered off. The cooled aqueous solution was extracted four times to remove any trace of dissolved 3,3′-dimethoxybenzyl. The dissolved ether and methanol were evaporated, and 200 mL of 10% sodium hydroxyde solution was added. The reaction mixture was then refluxed for 1 h, cooled in an ice bath, and acidified to pH 1.0 with cold 6 M HCl. The precipitated pyrrole was filtered off immediately and recrystallized from methanol−water (1:1) to give 1.5 g (22% yield) of **6a** as brown solid. ^{1}H NMR (DMSO): δ 12.70 (s, 2H, acid), 11.91

(11) Guilard, R.; Jérôme, F.; Gros, C. P.; Barbe, J.-M.; Ou, Z.; Shao, J.; Fischer, J.; Weiss, R.; Kadish, K. M. *Inorg. Chem.* **2001**, *40*, 4856−4865.
(12) Lin, X. Q.; Kadish, K. M. *Anal. Chem.* **1985**, *57*, 1498−1501.
(13) Ellis, J., P. E.; Linard, J. E.; Szymanski, T.; Jones, R. D.; Budge, J. R.; Basolo, F. *J. Am. Chem. Soc.* **1980**, *102*, 1889−1896.
(14) Rougee, M.; Brault, D. *Biochemistry* **1975**, *14*, 4100−4106.
(15) Barton, D. H. R.; Kervagoret, J.; Zard, S. Z. *Tetrahedron* **1990**, *46*, 7587−7598.
(16) Conlon, M.; Johnson, A. W.; Overend, W. R.; Rajapaksa, D. *J. Chem. Soc., Perkin Trans. 1* **1973**, 2281−2288.
(17) Hitchcock, P. B.; McLaughlin, G. M. *J. Chem. Soc., Dalton Trans.* **1976**, 1927−1930.

(s, 1H, NH), 7.12 (dd, 2H, $J_1 = J_2 = 5.6$ Hz, 5-anis.), 6.76 (d, 2H, $J = 5.6$ Hz, 6-anis.), 6.73 (d, 2H, $J = 5.6$ Hz, 4-anis.), 6.67 (s, 2H, 2-anis.), 3.63 (s, 6H, OMe). IR: ν 1675 cm^{-1} (CO). MS (EI): *m*/*z* (%) 367 (100) $[M]^+$, 323 $[M - CO_2]^{+\cdot}$, 305 $[M - 2OMe]^{+\cdot}$, 279 $[M - 2CO_2]^{+\cdot}$. Anal. Calcd for $C_{20}H_{17}NO_6,H_2O$: C, 62.32; H, 4.97; N, 3.64. Found: C, 62.34; H, 5.17; N, 3.57.

3,4-Di(*m*-anisyl)pyrrole (6b). A 3.0 g (8.2 mmol) amount of the diacid derivative **6a** was refluxed under argon in 75 mL of freshly distilled ethanolamine for 4 h. The hot ethanolamine solution was then poured into 200 mL of cold water and the aqueous solution extracted four times with 100 mL of methylene chloride. The combined organic layers were thoroughly washed with water in order to remove any trace of ethanolamine and then dried over magnesium sulfate. Evaporation of the solvent led to a crude solid which was recrystallized from methylene chloride−cyclohexane (1:1) to give 1.0 g of **6b** as a brown solid (yield 44%). ^{1}H NMR ($CDCl_3$): δ 8.38 (s, 1H, NH), 7.18 (d, 2H, $J = 7$ Hz, 6-anis.), 6.94 (s, 2H, 2-anis.), 6.91 (d, 2H, $J = 2.4$ Hz, 4-anis.), 6.88 (d, 2H, $J = 2$ Hz, α-free), 6.78 (dd, 2H, $J = 2.4$ and 7 Hz, 5-anis.), 3.70 (s, 6H, OMe). MS (EI): *m*/*z* (%) 279 (100) $[M]^{+\cdot}$. Anal. Calcd for $C_{18}H_{17}NO_2$: C, 77.38; H, 6.14; N, 5.02. Found: C, 77.48; H, 6.23; N, 5.32.

2-Formyl-3,4-di(*m*-anisyl)pyrrole (6c). In a typical experiment, 3,4-di(*m*-anisyl)pyrrole **6b** (2.1 g, 7.5 mmol) was dissolved, under argon and with shielding from light, in 100 mL of dry dimethylformamide (DMF). The solution was cooled to 0 °C by using an ice-water bath, and 4 mL of freshly distilled $POCl_3$ (43 mmol) was then slowly added. After addition, the stirring was kept at room temperature for 3 h after which the reaction mixture was poured into a 10% aqueous sodium hydroxyde solution (200 mL). The reaction mixture was refluxed for 1 h (under nitrogen), and the brown precipitate thus obtained was filtered off and washed thoroughly with water. Recrystallization from methanol led to **6c** as a brown solid (1.6 g, yield 69%).^{1}H NMR ($CDCl_3$): δ 9.94 (s, 1H, NH), 9.45 (s, 1H, CHO), 7.10−7.30 (m, anis.), 6.79−6.91 (m, anis.), 6.69 (d, 1H, α free), 3.71 (s, 3H, OMe), 3.62 (s, 3H, OMe). MS (EI): *m*/*z* (%) 307 (100) $[M]^{+\cdot}$, 279 $[M - CHO]^+$. Anal. Calcd for $C_{19}H_{17}NO_3$: C, 74.24; H, 5.58; N, 4.56. Found: C, 73.75; H, 5.57; N, 4.64.

2-Formyl-3,4-di(*p*-anisyl)pyrrole (7c). The title compound was prepared from **7b** (3.0 g, 10 mmol) using the above procedure described for **6c** ($m = 2.0$ g, yield 72%). ^{1}H NMR ($CDCl_3$): δ 9.93 (s, 1H, NH), 9.40 (s, 1H, CHO), 7.20 (d, 2H, $J = 8.8$ Hz, 2,6-anis.), 7.17 (d, 1H, $J = 2.9$ Hz, α-free), 7.07 (d, 2H, $J = 8.8$ Hz, 2,6-anis.), 6.87 (d, 2H, $J = 8.8$ Hz, 3,5-anis.), 6.77 (d, 2H, $J = 8.8$ Hz, 3,5-anis.), 3.82 (s, 3H, OMe), 3.77 (s, 3H, OMe). IR: ν 1639 cm^{-1} (CO). MS (EI): *m*/*z* (%) 307 $[M]^{+\cdot}$ (100). Anal. Calcd for $C_{19}H_{17}NO_3$: C, 74.24; H, 5.58; N, 4.56. Found: C, 74.11; H, 5.32; N, 4.44.

5,5′-Dicarboxy-3,3′-dimethyl-4,4′-diphenyldipyrryltoluene (11b). Benzaldehyde (1.70 g, 16 mmol) and pyrrole **5** (7.35 g, 32 mmol) were dissolved in absolute ethanol (170 mL). The mixture was refluxed under nitrogen, and 2.5 mL of concentrated HCl (12 M) was then added to the solution. The reflux was maintained for 1 h, and the reaction mixture was then evaporated on a rotary evaporator. During evaporation, a white solid precipitated which was further filtered off. The solid thus obtained was washed 3 times with cold methanol and dried. This diethyl ester derivative **11a** was not further purified and was used directly in the saponification step (4.4 g, yield 50.3%). ^{1}H NMR ($CDCl_3$): δ 9.32 (s, 2H, NH), 7.21−7.36 (m, 15H, Ph), 5.69 (s, 1H, CH), 4.00 (q, 4H, O−CH_2), 1.83 (s, 6H, Me), 0.99 (t, 6H, CH_3). MS (EI): *m*/*z* (%) 545 (100) $[M]^{+\cdot}$.

To a suspension of 4.3 g of the previously obtained triphenyldipyrromethane **11a** in absolute ethanol (200 mL) was added 1.8 g of sodium hydroxide dissolved in 10 mL of water. The reaction mixture was refluxed under argon, shielded from light for 4 h, and then cooled to room temperature. Acetic acid (500 mL) was then added until precipitation of a pink powder. The resulting solid was filtered, washed several times with water, and dried to give the title product **11b** (2.6 g, yield 67%). ^{1}H NMR ($CDCl_3$): δ 10.23 (s, 2H, COOH), 8.85 (s, 2H, NH), 7.14−7.43 (m, 15H, Ph), 5.70 (s, 1H, CH), 1.94 (s, 6H, Me).

7,8,12,13-Tetramethyl-2,3,10,17,18-pentaphenylcorrole (Me_4Ph_5-Cor)H_3 (8). 5,5′-Dicarboxy-4,4′-diethyl-3,3′-dimethyldipyrryltoluene (**3**) (4.72 g, 12.9 mmol) was dissolved in trifluoroacetic acid (200 mL) and the resulting orange solution was stirred for 10 min at room temperature. 3,4-Diphenyl-2-formylpyrrole (**4**) (7.0 g, 28.3 mmol) in methanol (500 mL) was added dropwise, and the red solution was stirred for 15 min. Evaporation of the solvent led to a green solid which was not further purified and used as a crude compound in the next reaction. *a*,*c*-Biladiene, previously obtained, was dissolved in methanol (1.00 L) saturated with sodium hydrogen carbonate and stirred at room temperature for 10 min. *p*-Chloranil (4.3 g) was then added, and the solution stirred for 15 min after which 43 mL of 50% hydrazine in water was added. After 15 min, the solvent was evaporated under vacuum to give a crude solid. The latter was redissolved in methylene chloride, washed with water, and dried with magnesium sulfate. Chromatography on basic alumina (methylene chloride elution) afforded the title product **7** ($m = 932$ mg, 12.7%), which corresponds to the first purple eluted compound. ^{1}H NMR ($CDCl_3$): δ 9.32 (s, 2H, *meso* 5, 15), 6.96−7.78 (m, 25H, Ph), 3.14 (s, 6H, Me), 2.21 (s, 6H, Me). UV−vis (CH_2Cl_2; λ_{max}, nm (ϵ, L mol^{-1} cm^{-1})): 419 (85 000), 567 (15 000), 607 (13 000), 640 (7000). MS (EI): *m*/*z* (%) 734 (100) $[M]^{+\cdot}$. Anal. Calcd for $C_{53}H_{42}N_4$: C, 86.61; H, 5.76, N, 7.63. Found: C, 86.25; H, 6.01; N, 7.60.

2,3,17,18-Tetra(*m*-anisyl)-7,8,12,13-tetramethyl-9-phenylcorrole (Me_4PhTm-$OCH_3PCor)H_3$ (9). This corrole was similarly prepared in 9% yield ($m = 105$ mg) from **3** ($m = 570$ mg, 1.56 mmol) and **6c** ($m = 1.0$ g, 3.2 mmol). ^{1}H NMR ($CDCl_3$): δ 9.40 (s, 2H, meso 5, 15), 7.93 (d, 2H, $J = 6$ Hz, 2,6-Ph), 7.69 (m (dd+s), 2H, 3,4,5-Ph), 7.49 (d, 2H, $J = 5$ Hz, 4-anis.), 7.30 (d, 2H, $J = 3$ Hz, 4-anis.), 7.11 (d, 2H, $J = 6$ Hz, 6-anis.), 6.99 (m, 8H, 6-anis., 5-anis., 2 × 2-anis.), 6.59 (dd, 2H, $J = 3$ and 6 Hz, 5-anis.), 3.74 (s, 6H, OMe), 3.62 (s, 6H, OMe), 3.18 (s, 6H, Me), 2.23 (s, 6H, Me). UV−vis (CH_2Cl_2; λ_{max}, nm (ϵ, L mol^{-1} cm^{-1})): 410 (63 000), 422 (71 000), 535 (13 000), 566 (16 000), 607 (14 000), 638 nm (8000). MS (EI): *m*/*z* (%) 854 (100) $[M]^{+\cdot}$. Anal. Calcd for $C_{57}H_{50}N_4O_4$, MeOH: C, 78.52; H, 6.14; N, 6.32. Found: C, 79.00; H, 6.51; N, 6.36.

2,3,17,18-Tetra(*p*-anisyl)-7,8,12,13-tetramethyl-9-phenylcorrole (Me_4PhTp-$OCH_3PCor)H_3$ (10). This corrole was similarly prepared in 20% yield ($m = 450$ mg) from **3** ($m = 1.0$ g, 2.74 mmol) and **7c** ($m = 1.7$ g, 5.5 mmol). ^{1}H NMR ($CDCl_3$): δ 9.31 (s, 2H, meso 5, 15), 7.95 (d, 2H, $J = 5$ Hz, 2,6-Ph), 7.77 (dd, 2H, $J = 4$ and 5 Hz, 3,5-Ph), 7.67 (d, 1H, $J = 4$ Hz, 4-Ph), 7.37 (d, 4H, $J = 8.5$ Hz, 2,6-anis.), 7.12 (d, 4H, $J = 9.1$ Hz, 2,6-anis.), 6.95 (d, 4H, $J = 8.5$ Hz, 3,5-anis.), 6.53 (d, 4H, $J = 9.1$ Hz, 3,5-anis.), 3.95 (s, 6H, OMe), 3.79 (s, 6H, OMe), 3.15 (s, 6H, Me), 2.22 (s, 6H, Me). UV−vis (CH_2Cl_2; λ_{max}, nm (ϵ, L mol^{-1} cm^{-1})): 413 (70 000), 422 (73 000), 520 (16 000), 559 (16 000), 609 (13 000), 638 nm (8000). MS (EI): *m*/*z* (%) 854 (100) $[M]^{+\cdot}$. Anal. Calcd for $C_{57}H_{50}N_4O_4$, MeOH: C, 78.52; H, 6.14; N, 6.32. Found: C, 78.22; H, 5.92; N, 6.56.

8,12-Dimethyl-2,3,7,10,13,17,18-heptaphenylcorrole (Me_2Ph_7Cor)-H_3 (12). This corrole was similarly prepared in 11.2% yield ($m = 285$ mg) from **11b** ($m = 1.584$ g, 3.23 mmol) and **4** ($m = 1.58$ g, 6.39 mmol). ^{1}H NMR ($CDCl_3$): δ 9.32 (s, 2H, meso 5, 15), [6.62−7.85] (m, 35H, Ph), 3.05 (s, 6H, Me). UV−vis (CH_2Cl_2; λ_{max}, nm (ϵ, L mol^{-1} cm^{-1})): 418 (62 000), 426 (62 000), 567 (15 000), 611 (12 000). MS (EI): *m*/*z* (%) 858 (100) $[M]^{+\cdot}$. Anal. Calcd for $C_{63}H_{46}N_4$, MeOH: C, 86.25; H, 5.66; N, 6.29. Found: C, 86.51; H, 5.91; N, 6.53.

Synthesis of Cobalt Derivatives. Synthesis of the various cobalt corroles was carried out as described below:

(8,12-Diethyl-7,13-dimethyl-2,3,17,18-tetraphenylcorrolato)-cobalt(III), ($Me_2Et_2Ph_4Cor$)Co (14). A solution of 50 mg (0.058 mmol) of ($Me_2Et_2Ph_4Cor$)H_3 (**2**) and 120 mg of $Co(OAc)_2{\cdot}4H_2O$ in 40 mL of dimethylformamide was heated under argon at 50 °C for 10 min. The solvent was then evaporated in a vacuum, and the residue was passed through a column of alumina using methylene chloride as eluent. After crystallization from methylene chloride−methanol (1:1), the title compound was obtained in 20% yield (11 mg). UV−vis (CH_2Cl_2; λ_{max}, nm (ϵ, L mol^{-1} cm^{-1})): 394 (66 000), 526 (15 000). MS (EI): *m*/*z* (%) 742 (100) $[M]^{+\cdot}$. Anal. Calcd for $C_{49}H_{39}N_4Co$, MeOH: C, 77.49; H, 5.60; N, 7.23. Found: C, 77.39; H, 5.48; N, 7.47.

(7,8,12,13-Tetramethyl-2,3,10,17,18-pentaphenylcorrolato)-cobalt(III), (Me_4Ph_5Cor)Co (15). This corrole was similarly prepared in 20% yield from 50 mg of (Me_4Ph_5Cor)H_3 (**8**) and 120 mg of $Co(OAc)_2{\cdot}4H_2O$. UV−vis (CH_2Cl_2; λ_{max}, nm (ϵ, L mol^{-1} cm^{-1})): 398

(45 000), 529 (11 000). MS (EI): *m*/*z* (%) 789 (100) $[M]^{+\cdot}$. Anal. Calcd for $C_{53}H_{39}N_4Co$, MeOH: C, 78.81; H, 5.27; N, 6.81. Found: C, 78.87; H, 5.26; N, 6.60.

(2,3,17,18-Tetra(*m*-anisyl)-7,8,12,13-tetramethyl-9-phenylcorrolato)cobalt(III) (Me_4PhTm-OCH_3PCor)Co (16). This corrole was similarly prepared in 31% yield from 50 mg of (Me_4PhTm-OCH_3PCor)-H_3 (**9**) and 120 mg of $Co(OAc)_2 \cdot 4H_2O$. UV−vis (CH_2Cl_2; λ_{max}, nm (ϵ, L mol^{-1} cm^{-1})): 404 (52 000), 533 (17 000). MS (EI): *m*/*z* (%) 909 (100) $[M]^{+\cdot}$. Anal. Calcd for $C_{57}H_{47}N_4O_4Co$, MeOH: C, 73.88; H, 5.41; N, 5.94. Found: C, 73.80; H, 5.74; N, 5.72.

(2,3,17,18-Tetra(*p*-anisyl)-7,8,12,13-tetramethyl-9-phenylcorrolato)cobalt(III) (Me_4PhTp-OCH_3PCor)Co (17). This corrole was similarly prepared in 31% yield from 200 mg of (Me_4PhTp-OCH_3-$PCor)H_3$ (**10**) and 480 mg of $Co(OAc)_2 \cdot 4H_2O$. UV−vis (CH_2Cl_2; λ_{max}, nm (ϵ, L mol^{-1} cm^{-1})): 398 (59 000), 533 (16 000). MS (EI): *m*/*z* (%) 909 (100) $[M]^{+\cdot}$. Anal. Calcd for $C_{57}H_{47}N_4O_4Co$, MeOH: C, 73.88; H, 5.41; N, 5.94. Found: C, 74.33; H, 5.44; N, 6.12.

(8,12-Dimethyl-2,3,7,10,13,17,18-heptaphenylcorrolato)-cobalt(III) (Me_2Ph_7Cor)Co (18). This corrole was similarly prepared in 21% yield from 100 mg of ($Me_2Ph_7Cor)H_3$ (**12**) and 250 mg of $Co(OAc)_2 \cdot 4H_2O$. UV−vis (CH_2Cl_2; λ_{max}, nm (ϵ, L mol^{-1} cm^{-1})): 406 (53 000), 538 (14 000). MS (EI): *m*/*z* (%) 911 (100) $[M]^{+\cdot}$. Anal. Calcd for $C_{57}H_{47}N_4Co$, MeOH: C, 81.33; H, 4.80; N, 5.93. Found: C, 81.57; H, 5.12; N, 6.23.

Crystallographic Determination of (Me_4Ph_5Cor)$Co(py)_2$. Single crystals of (Me_4Ph_5Cor)$Co(py)_2 \cdot 3CH_2Cl_2 \cdot H_2O$ suitable for X-ray diffraction were obtained by slow diffusion of methanol into a concentrated dichloromethane solution of **15** containing a few drops of pyridine. Data were collected on a Nonius KappaCCD diffractometer at −100 °C using Mo−Kα graphite monochromated radiation ($\lambda = 0.7107$ Å), ϕ scans. The structure was solved using direct methods and refined against $|F|$. For all computations the OpenMoleN package[18] was used.

Crystal Data for (Me_4Ph_5Cor)$Co(py)_2 \cdot 3CH_2Cl_2 \cdot H_2O$. Dark red crystals, crystal dimensions 0.20 × 0.15 × 0.10 mm: $C_{129}H_{106}Cl_6Co_2N_{12}O = 2(C_{63}H_{49}CoN_6) \cdot 3CH_2Cl_2 \cdot H_2O$, $M = 2170.95$, orthorhombic, space group $Pna2_1$, $a = 19.5690(4)$ Å, $b = 17.1070(6)$ Å, $c = 15.9160(6)$ Å, $V = 5328.2(5)$ Å^3, $Z = 2$, $D_c = 1.35$ g cm^{-3}, μ(Mo−Kα) = 0.522 mm^{-1}. A total of 35 460 reflections were collected, $2.5° < \theta < 30.5°$, 4791 independent reflections having $I > 3\sigma(I)$, 693 parameters. One of the three CH_2Cl_2 molecules is disordered with a water molecule. All non-hydrogen atoms were refined anisotropically. The hydrogen atoms, with the exception of CH_2Cl_2 and water protons, were introduced as fixed contributors ($d_{C-H} = 0.95$ Å, $B_H = 1.3B_{equ}$(C) Å^2). The absolute structure was determined by refining Flack's *x* parameter. Final results $R(F) = 0.069$, $R_w(F) = 0.083$, GOF = 1.488, maximum residual electronic density 0.971 e Å^{-3}. Data for this structure have been deposited with the Cambridge Crystallographic Data Centre as Supplementary publication no. CCDC-168247.

Results and Discussion

Synthesis of Aryl Substituted Corroles. The synthesis of 3,4-di(phenyl)- and 3,4-di(*p*-anisyl)pyrroles was performed as described in the literature starting from benzyl and dimethyl *N*-acetyliminodiacetate in the presence of sodium methoxide, followed by decarboxylation in refluxing ethanolamine.[19] A similar procedure was used to access the 3,4-di(*m*-anisyl)pyrrole, **6a**. Standard Vilsmeier−Haack formylation of 3,4-di(aryl)-pyrrole **6b** or **7b** with 1 equiv of Vilsmeier reagent ($POCl_3$/DMF), followed by recrystallization, resulted in the isolation of 2-formylpyrroles **6c** and **7c** in 69 and 72% yield, respectively (Scheme 1).

The free base aryl substituted corroles **8**−**10** were obtained in only two steps by condensation of 2 equiv of the corresponding formylpyrrole (**4**, **6c,** or **7c**) with 5-phenyldipyrromethane (**3**) as described in Scheme 2. The *a*,*c*-biladiene formed as an intermediate was not isolated and used as obtained in the cyclization reaction, this later step being carried out by the in-situ addition of sodium hydrogen carbonate and *p*-chloranil, followed by addition of 50% hydrazine in water. The crude corroles were further purified by column chromatography after solvent removal.

Scheme 1

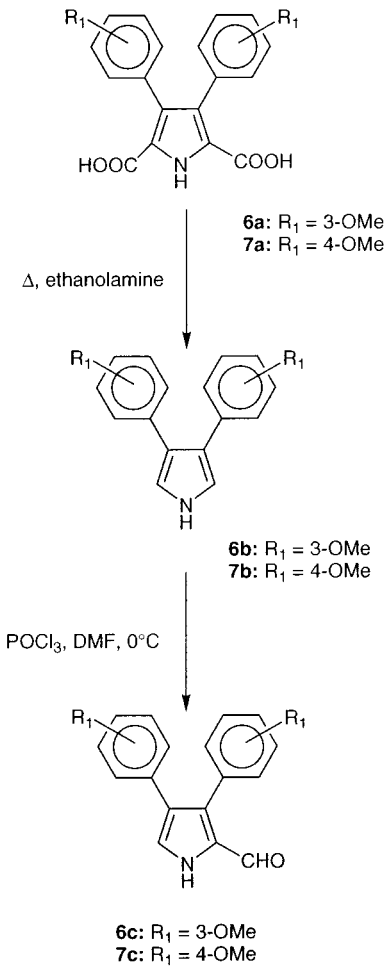

Heptaphenyl corrole, **12**, was similarly prepared except that its synthesis required a symmetrical triphenyldipyrromethane, **11b**, which was first obtained by acid-catalyzed condensation of **5** with benzaldehyde (Scheme 3). The asymmetrical ethyl 4-methyl-3-phenyl-*1H*-pyrrole-2-carboxylate (**5**) was synthesized as described in the literature[20] by base-catalyzed condensation of nitroethane to benzaldehyde, followed by subjecting the resulting phenylnitropropene derivative to the Barton−Zard pyrrole synthesis conditions ($CNCH_2CO_2Et$, THF, Pr^iOH, DBU).[15]

The isolated yield of the sterically hindered arylcorroles ranges from 10 to 12.5% except for **9** which was isolated in 9% yield; the low yield observed in the case of **9** may suggest steric hindrance of the *m*-methoxy group in the cyclization step.

The proton NMR spectra of the free base corroles **8**−**10** and **12** show a singlet corresponding to the *meso* protons between 9.30 and 9.40 ppm, whereas the aryl groups (phenyl and anisyl) appear as multiplets in the range of 6.50−7.93 ppm. The methyl groups resonate as a singlet at 2.22 ppm.

Mass spectra exhibit similar characteristics for each free base derivative. The parent peak corresponds in all cases to the

(18) *OpenMoleN, Interactive Structure Solution*; Nonius B. V.: Delft, The Nederlands, 1997.
(19) Friedman, M. *J. Org. Chem.* **1965**, *30*, 859−863.
(20) Dumoulin, H.; Rault, S.; Robba, M. *J. Heterocycl. Chem.* **1997**, *34*, 13−16.

Scheme 2

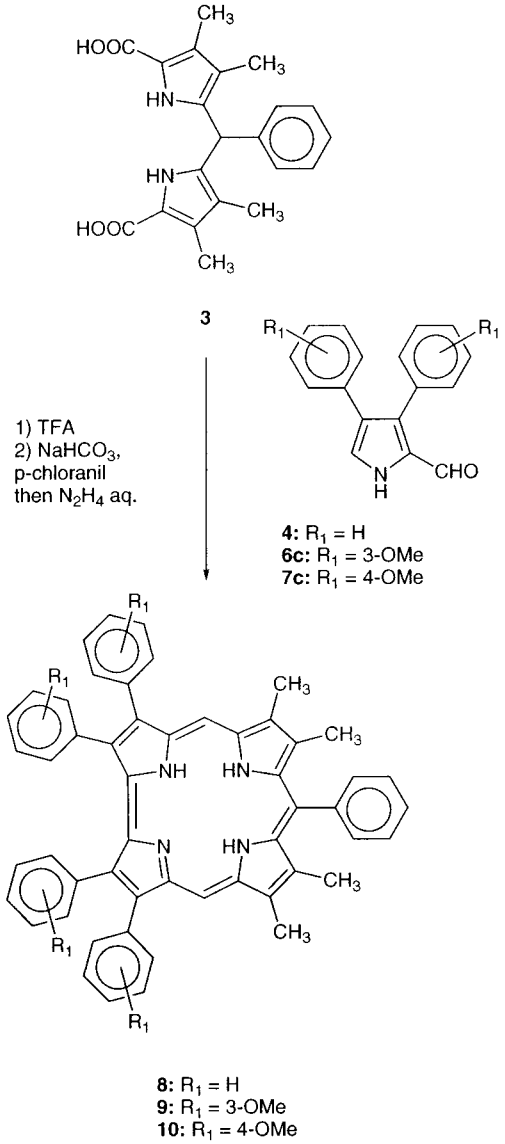

Scheme 3

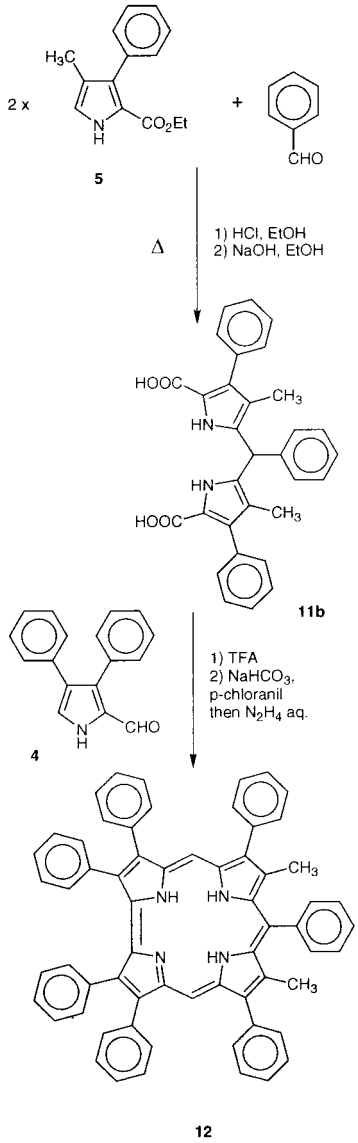

molecular ion $[M]^{\bullet+}$. The Soret bands of the phenyl substituted derivatives are red-shifted as compared to the well-known free base $(Me_6Et_2Cor)H_3$, **1**, due to the ring current decrease generated by the phenyl substituents (see Table 1).

The metallocorroles **13**−**18** (see Chart 1) were synthesized according to literature procedures[7,16,17,21] which involved reaction of cobalt(II) acetate tetrahydrate with the corresponding free base corrole in DMF at 50 °C, the metalation reaction in this case being monitored by UV−visible spectroscopy. The reaction was complete within 10−15 min as indicated by disappearance of the characteristic free base absorption at 591−611 nm (see Table 1). The isolated yields of the cobalt corroles varied from 20 to 31%, as given in the Experimental Section.

The main features of the electronic absorption spectra for the investigated cobalt(III) corroles in nonbonding media under N_2 are two intense absorptions, one of which is centered at 381−406 nm and the other at 502−538 nm (see Experimental Section). The parent peak of the mass spectra corresponds in each case to the molecular ion $[M]^{\bullet+}$.

Structure of $(Me_4Ph_5Cor)Co(py)_2$. Top and side views of the molecular structure of $(Me_4Ph_5Cor)Co(py)_2$ are displayed in Figure 1a,b, together with the labeling scheme used for all non-hydrogen atoms. Crystal data for $(Me_4Ph_5Cor)Co(py)_2 \cdot 3CH_2Cl_2 \cdot H_2O$ and details of the diffraction data collection are given in Table 2. Selected bond distances and angles found in $(Me_4Ph_5Cor)Co(py)_2$ are given in Table 3.

The six-coordinate, low-spin central cobalt atom is bound to six nitrogen atoms, four pyrrole nitrogens N_p belonging to the corrole ring and two axial pyridine−nitrogens N_{py} (Figure 1). The four $Co-N_p$ bond lengths range from 1.884(6) to 1.915(6) Å, leading to an average bond distance of 1.894(6) Å. Although, not significantly different from the other $Co-N_p$ bond distances, the two shortest $Co-N_p$ bond lengths of 1.884(6) and 1.886(6) Å correspond to the $Co-N_p$ bonds involving the two N_p atoms belonging to the two pyrrole rings linked directly via a $C_\alpha-C_\alpha$ bond. Similar features have been previously observed in the structures of other metallocorroles.[1,2] The average value of the two axial $Co-N_{py}$ bond distances (1.991(7) Å) is slightly longer than the mean value of the four $Co-N_p$ distances (1.894(6) Å). These $Co-N_p$ and axial $Co-N_{py}$ bond distances are significantly shorter than the corresponding ones present in the low-spin, six-coordinate cobalt(III) bis-piperidine complex, $[(TPP)Co(pip)_2]^+$, where the average $Co-N_p$ and $Co-N_{pip}$ bond distances are

(21) Paolesse, R.; Licoccia, S.; Fanciullo, M.; Morgante, E.; Boschi, T. *Inorg. Chim. Acta* **1993**, *203*, 107−114.

Table 1. Selected Absorption Maxima and Molar Absorptivities of Representative Free Base Corroles in CH_2Cl_2

compound	Soret bands		λ_{max}, nm ($\epsilon \times 10^4$, L mol^{-1} cm^{-1})	Visible bands		
$(Me_6Et_2Cor)H_3$[a] **(1)**	395 (12.9)	406 (9.9)	535 (1.5)	549 (1.5)	591 (1.9)	
$(Me_2Et_6Cor)H_3$[b]	395 (12.7)	407 (10.1)	537 (1.9)	549 (1.9)	593 (2.4)	
$(Me_2Et_6PhCor)H_3$[c]	401 (7.3)	413 (7.0)	546 (1.0)	555 (1.0)	598 (1.0)	
$(Me_2Et_2Ph_4Cor)H_3$ **(2)**[d]	400 (8.3)	413 (7.5)		564 (1.9)	599 (2.1)	
$(Me_4Ph_5Cor)H_3$ **(8)**		419 (8.5)		567 (1.5)	607 (1.3)	640 (0.7)
$(Me_4Ph(m\text{-}OMePh)_4Cor)H_3$ **(9)**	410 (6.3)	422 (7.1)	535 (1.3)	566 (1.6)	607 (1.4)	638 (0.8)
$(Me_4Ph(p\text{-}OMePh)_4Cor)H_3$ **(10)**	413 (7.0)	422 (7.3)	520 (1.6)	559 (1.6)	609 (1.3)	
$(Me_2Ph_7Cor)H_3$ **(12)**	418 (6.2)	426 (6.2)		567 (1.5)	611 (1.2)	

[a] Grigg, R.; Johnson, A. W.; Shelton, G. *J. Chem. Soc. C* **1971**, 2287−2294. [b] Tardieux, C. Ph.D. Thesis, Université de Bourgogne, Dijon, France, 1997. [c] Data taken from ref 6. [d] Data taken from ref 7.

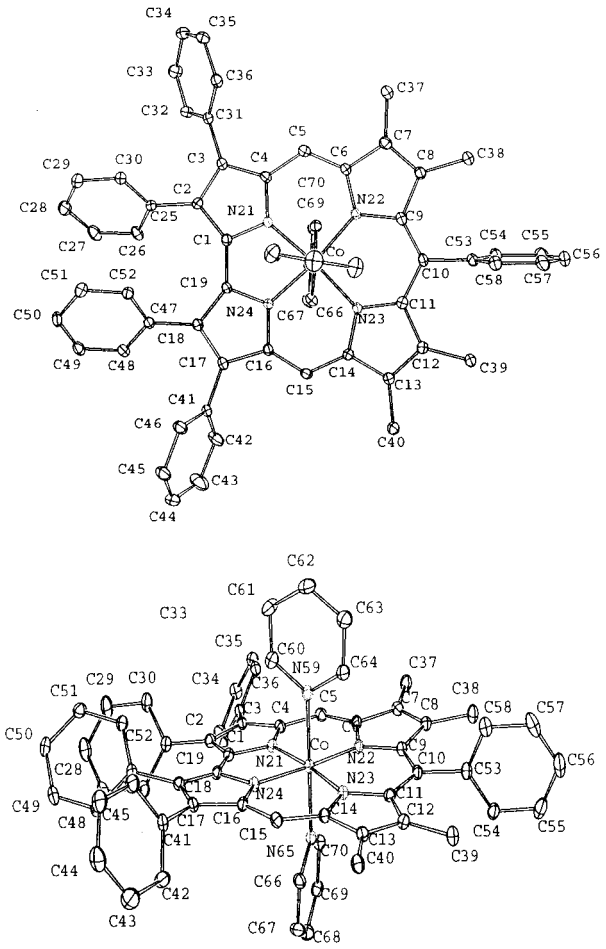

Figure 1. ORTEP diagrams of $(Me_4Ph_5Cor)Co(py)_2$ (top) top-view and (bottom) side view. Thermal ellipsoids are drawn to illustrate 30% probability surfaces.

1.979 and 2.060 Å, respectively.[22] The shortening of the Co−N_p bond lengths in the corrole derivative $(Me_4Ph_5Cor)Co(py)_2$ can be ascribed to the reduced hole size of the corrole ligand $[Me_4Ph_5Cor]^{3-}$ relative to the tetraphenylporphyrin ligand $[TPP]^{2-}$, since a similar decrease of the M−N_p bond lengths was observed in several other metallocorroles as different as $(Me_8Cor)Rh(AsPh_3)$,[23] $(Me_8Ph_3Cor)Co(PPh_3)$[9] (Cor = β-unsubstituted corrole ring; Me_8Ph_3Cor = 5,10,15-triphenyl-2,3,7,8,12,13,17,18-octamethylcorrole), and $(Me_8Cor)Mn$.[24]

Table 2. Crystal Data and Structure Refinement Parameters for $(Me_4Ph_5Cor)Co(py)_2.3CH_2Cl_2.H_2O$

formula	$C_{129}H_{106}Cl_6Co_2N_{12}O$-$2(C_{63}H_{49}CoN_6)\cdot 3CH_2Cl_2\cdot H_2O$
MW	2170.95
cryst syst	orthorhombic
space group	$Pna2_1$
a (Å)	19.5690(4)
b (Å)	17.1070(6)
c (Å)	15.9160(6)
V (Å^3)	5328.2(5)
Z	2
color	dark red
cryst dimen (mm)	0.20 × 0.15 × 0.10
D_{calc} (g cm^3)	1.35
F(000)	2256
μ (mm^{-1})	0.522
temp (K)	173
wavelength (Å)	0.710 73
radiation	Mo Kα graphite monochromated
diffractometer	KappaCCD
scan mode	ϕ scans
hkl limits	0,22/0,24/0,21
Θ limits (deg)	2.5/30.51
no. of data measrd	35 460
no. data with $I > 3\sigma(I)$	4791
weighting scheme	$4F_o^2/(\sigma^2(F_o^2) + 0.0004F_o^4) + 1.0$
no. of variables	693
R	0.069
R_w	0.083
GOF	1.488
largest peak in final difference (e Å^3)	0.971

Table 3. Selected Interatomic Distances (Å) and Angles (deg) for $(Me_4Ph_5Cor)Co(py)_2$.

Bond Lengths (Å)			
Co−N21	1.886(6)	<Np−Cα>	1.378(8)
Co−N22	1.915(6)	<Cα−Cβ>	1.441(8)
Co−N23	1.892(6)	<Cβ−Cβ>	1.385(8)
Co−N24	1.884(5)	<Cmeso−Cα>	1.402(9)
<Co−Np>	1.894(5)	<Cβ−Cphen>	1.484(9)
Co−N59	1.980(7)	<Cβ−Cmet>	1.503(9)
Co−N65	2.003(7)	<Cphe−Cphe>	1.386(9)
Angles (deg)			
<Cα−Np−Cα>	109.2(5)	<Cα−Cmeso−Cα>	124.6(6)
<Np−Cα−Cβ>	108.0(5)	<Np−Cα−Cmeso>	123.2(6)
<Cα−Cβ−Cβ>	107.4(5)	<Cphe−Cphe−Cphe>	120.0(9)

The central cobalt atom in $(Me_4Ph_5Cor)Co(py)_2$ lies almost in the 23-atom core corrole mean plane. Its displacement of 0.002(1) Å relative to this mean plane is not significant. It lies also at 0.021(1) Å above the $4N_p$ mean plane. The location of the cobalt atom in the corrole mean plane is probably related to its six-coordination, that is, the presence of the two axial pyridine molecules bound to the central metal. In the five-coordinate cobalt(III) corrole derivatives of known structures,[9,17] a larger displacement of the metal atom away from the 23-atom core mean plane is observed. In the two previously characterized five-coordinate triphenylphosphine cobalt(III) corrole com-

(22) Scheidt, W. R.; Cunningham, J. A.; Hoard, J. L. *J. Am. Chem. Soc.* **1973**, *95*, 8289−8294.
(23) Boschi, T.; Liccocia, S.; Paolesse, R.; Tagliesta, P.; Tehran, M. A.; Pelizzi, G.; Vitali, F. *J. Chem. Soc., Dalton Trans.* **1990**, 463−468.
(24) Liccocia, S.; Morgante, E.; Paolesse, R.; Polizio, F.; Senge, M. O.; Tondello, E.; Boschi, T. *Inorg. Chem.* **1997**, *36*, 1564−1570.

Table 4. Half-Wave Potentials (V vs SCE) of Mono-Cobalt Corroles in CH_2Cl_2, 0.1 M TBAP

	red	ox				
compound	first	fourth	third	second	first	Δox(2−1)
(Me_6Et_2Cor)Co (**13**)	−0.31	1.21	1.07	0.59	0.03	0.62
(Et_8Cor)Co[a]	−0.30	1.17	0.94	0.57	0.11	0.46
($Me_2Et_2Ph_4$Cor)Co (**14**)	−0.16	1.25	0.94	0.76	0.30	0.46
(Me_2Ph_7Cor)Co (**18**)	*b*	1.26	0.84	0.52	0.34	0.18
(Me_4Ph(*p*-OMePh)$_4$Cor)Co (**17**)	−0.18	1.15	0.87	0.55	0.38	0.17
(Me_4Ph(*m*-OMePh)$_4$Cor)Co (**16**)	−0.15	1.24	0.85	0.59	0.42	0.17
(Me_4Ph_5Cor)Co (**15**)	−0.15	1.26	0.87	0.62	0.45	0.17

[a] Data are taken from ref 10. [b] Broad irreversible process.

plexes, the displacement of the cobalt atom relative to the corrole mean plane is 0.38 Å in (Cor)Co(PPh_3)[17] and 0.29 Å in (Me_8-Ph_3Cor)Co(PPh_3).[9] It should also be noted that the two pyridine molecules are almost perpendicular to the corrole mean plane (84.6(2) and 89.4(2)°), while the dihedral angle between the two axial pyridine molecule mean planes is equal to 83.7(2)° (Figure 1).

The corrole core is essentially planar. The maximum displacement of the carbon and nitrogen atoms relative to corrole mean plane is 0.20(1) Å (C7), whereas the average displacement of the carbon and nitrogen atoms from this mean plane is only 0.09(1) Å. The small perpendicular displacements of the geminal β-carbons above and below the corrole mean plane show that a very small saddling of the core is present. The average displacements of the geminal β-carbons corresponding to the methylated and phenylated pyrroles above and below the corrole mean plane are 0.16(1) and 0.19(1) Å, respectively. Moreover, very small ruffling and doming distortions are superimposed to the saddle deformation, as indicated by the average displacements of the *meso*-carbons above and below the corrole core mean plane of 0.02(1) and − 0.07(1) Å and the position of the $4N_p$ mean plane which lies only 0.023(1) Å above the corrole-core mean plane. Despite a larger steric crowding in this six-coordinate cobalt(III) species, (Me_4Ph_5Cor)Co($py)_2$, the overall conformation of the corrole core is comparable to that present in the two five-coordinate triphenylphosphine cobalt(III) corroles, (Cor)Co(PPh_3)[17] and (Me_8Ph_3Cor)Co(PPh_3),[9] where the average displacements of the carbon and nitrogen atoms away from the corrole mean planes are 0.05 and 0.14 Å, respectively.

No unusual intermolecular short distances occur in the crystals of (Me_4Ph_5Cor)Co($py)_2$·$3CH_2Cl_2$·H_2O.

Electrochemistry. The Co(III)/Co(II) reaction is reversible for five of the six investigated compounds. This reduction occurs at $E_{1/2} = -0.30$ or -0.31 V for the two derivatives with only ethyl or methyl substituents ((Et_8Cor)Co and compound **13**) and the potentials are shifted to an easier reduction located at $E_{1/2} = -0.15$ to -0.18 V for the corroles with four or five phenyl substituents at the β- or *meso*-positions of the macrocycle (compounds **14**−**17**) (see Table 4). An irreversible Co(III)/Co(II) process is seen for (Me_2Ph_7Cor)Co (compound **18**), as indicated by broad reduction and reoxidation peaks which are separated by 350 mV for a scan rate of 0.1 V/s.

Similar UV−visible changes are observed during controlled-potential electroreduction of compounds **13**−**17** and an example of the thin-layer spectral changes is shown in Figure 2a for the case of (Me_4Ph_5Cor)Co (**15**). The initial Co(III) corroles are all characterized by a single absorption band in the visible region of the spectrum ($\lambda_{max} = 529$ nm for **15**), while the Co(II) reduction products each have two well-defined visible bands, one of which is located between 535 and 561 nm and the other between 574 and 641 nm (Table 5 and Figure 2a). The spectrum of compound **13**, which contains only alkyl substituents, differs

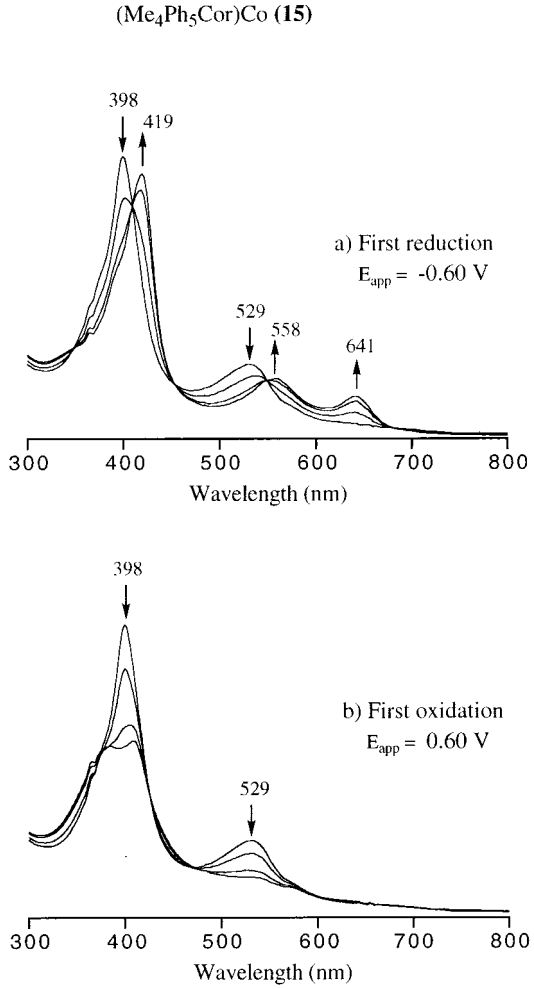

Figure 2. UV−visible spectral changes during thin-layer controlled-potential electrolysis of (Me_4Ph_5Cor)Co (**15**) at (a) −0.60 and (b) +0.60 V in CH_2Cl_2, 0.1 M TBAP.

substantially in its neutral and reduced forms from that of compounds **14**−**18**, all of which contain phenyl groups at the β-pyrrole positions of the macrocycle. The thin-layer spectral changes obtained upon reduction of compound **13** are reversible and almost identical to spectral changes which have been reported upon the metal-centered reduction of other Co(III) corroles under similar solution conditions.[1,2,10,25]

The electrooxidation of each cobalt corrole was also investigated by cyclic voltammetry in CH_2Cl_2 containing 0.1 M TBAP. The redox potentials for these processes are summarized in Table 4 and examples of cyclic voltammograms for compounds **13**−**15** and (Et_8Cor)Co are shown in Figure 3 which is arranged from the most difficult to reduce and easiest to oxidize

(25) Adamian, V. A. Ph.D. Dissertation, University of Houston, TX, 1995.

Table 5. UV−Visible Spectral Data for Co(III) and Co(II) Corroles in CH_2Cl_2 Containing 0.1 M TBAP

cpd	metal ion	λ_{max}, nm ($\epsilon \times 10^4$, L mol^{-1} cm^{-1})								
		CH_2Cl_2 under N_2			**C**H_2Cl_2 under CO			pyridine under N_2		
13	Co(III)	381 (7.6)	502 (0.9)		378(4.3)	540(1.2)		425(4.8)	538(0.9)	576(2.9)
14		394 (6.6)	526 (1.5)		393(4.8)	562(1.7)		428(5.0)	547(0.9)	593(3.0)
15		398 (4.5)	529 (1.1)		407(3.3)	567(1.3)		433(3.5)	557(0.7)	598(1.7)
16		404 (5.2)	533 (1.7)		406(4.2)	564(1.6)		435(4.2)	554(0.9)	598(2.0)
17		398 (5.9)	533 (1.6)		395(3.9)	564(1.7)		433(3.8)	553(0.8)	598(2.3)
18		406 (5.3)	538 (1.4)		409(3.9)	562(1.5)		442(4.1)	558(0.8)	598(1.5)
13	Co(II)	405 (8.1)	535 (1.2)	574 (0.9)						
14		415 (7.0)	553 (1.1)	612 (0.9)						
15		419 (4.4)	558 (1.0)	641 (0.7)						
16		423 (5.4)	559 (1.5)	641 (0.9)						
17		423 (5.4)	559 (1.3)	641 (1.1)						
18		429 (4.7)	561 (1.4)	641 (1.1)						

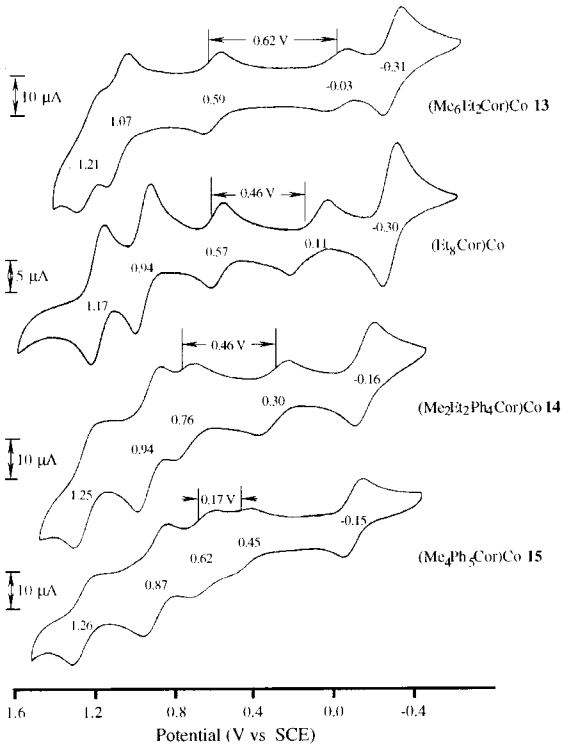

Figure 3. Cyclic voltammograms of 2.0×10^{-3} M (Me_6Et_2Cor)Co (**13**), 3.0×10^{-3} M (Et_8Cor)Co, 2.0×10^{-3} M ($Me_2Et_2Ph_4$Cor)Co (**14**), and 1.5×10^{-3} M (Me_4Ph_5Cor)Co (**15**) in CH_2Cl_2, 0.1 M TBAP.

compound (**13**) to the derivative which is easiest to reduce and hardest to oxidize of the four compounds (**15**). The electrochemistry of (Et_8Cor)Co was earlier characterized under similar solution conditions.[10]

The electrochemistry of compounds **13**−**18** in CH_2Cl_2 is similar to what has been reported for (Et_8Cor)M where M = Co, Ni, or Cu in noncoordinating or weakly coordinating media.[10] The formally M(III) complexes are all monomeric in their neutral and singly reduced forms, but all are proposed to exist as $\pi-\pi$ dimers which are formulated as $[(Et_8Cor)M]_2^+$ and $[(Et_8Cor)M]_2^{2+}$ after the first two one-electron oxidations in CH_2Cl_2. The cyclic voltammograms of (Et_8Cor)M under these solution conditions exhibit four reversible oxidation processes, the first two of which involve the abstraction of one electron per two metallocorrole units and have peak currents which are only half as large as seen for the other electron-transfer processes. Compounds **13**−**18** also exhibit five sets of oxidation/reduction peaks or four sets of oxidation peaks in CH_2Cl_2 (see Table 4), and in each case the diffusion controlled peak currents for the first two oxidations are approximately half the values seen for the other three redox reactions (see Figure 3).

The thin-layer spectral changes obtained during the first oxidation of compounds **13**−**18** are similar to each other, and an example of the thin-layer UV−visible spectroelectrochemical data is shown in Figure 2b for the case of (Me_4Ph_5Cor)Co (**15**) where the first oxidation product at an applied potential of +0.60 V is formulated as $[(Me_4Ph_5Cor)Co]_2^+$.

One key feature in the voltammograms of compounds **13**−**18** is the absolute potential separation between $E_{1/2}$ values for the first and second oxidations, Δox(2−1). The Δox(2−1) values are indicated in Figure 3 and summarized in the last column of Table 4 for each compound. These values range from 0.62 V for compound **13** to a smaller separation of 0.17−0.18 V for compounds **15**−**18**, all four of which contain a phenyl group at the 10-*meso* position of the corrole macrocycle.

The larger Δox(2−1) values can be associated with a stronger interaction between the two equivalent redox centers in the singly oxidized compound,[10,26−29] and the data suggest the following order of interaction between the half-oxidized corrole dimers.

$$[(Me_6Et_2Cor)Co]_2^+ > [(Et_8Cor)Co]_2^+ \approx [\mathbf{14}]_2^+ > [\mathbf{15}]_2^+ \approx [\mathbf{16}]_2^+ \approx [\mathbf{17}]_2^+ \approx [\mathbf{18}]_2^+$$

A detailed electrochemical study of dimer formation as a function of solvent and corrole macrocyclic structure will be published elsewhere,[30] but it should now be clearly noted that all of the presently examined corroles exist as unaggregated monomers in their neutral or singly reduced forms.

Formation of Mono- and Bis-Pyridine Adducts. Each cobalt corrole was investigated as to its pyridine binding ability in CH_2Cl_2/pyridine mixtures. The addition of pyridine to a CH_2Cl_2 solution of each corrole leads initially to a decrease in intensity of the Soret and visible band of the neutral complex, and this is followed at higher pyridine concentrations by a large red shift of the Soret band and the appearance of a new intense

(26) (a) Geiger, W. E.; Connelly, N. G. In *Advances in Organometallic Chemistry*; Stone, F. G. A., West, R., Eds.; Academic: Orlando, FL, 1985; Vol. 24, pp 89−97. (b) Kotz, J. C. In *Topics in Organic Electrochemistry*; Fry, A. J., Britton, W. E., Eds.; Plenum: New York, 1986; pp 95−109.
(27) Yap, W. T.; Durst, R. A. *J. Electroanal. Chem. Interfacial Electrochem.* **1981**, *130*, 3.
(28) Kadish, K. M.; Boulas, P.; D'Souza, F.; Aukauloo, M. A.; Guilard, R.; Lausmann, M.; Vogel, E. *Inorg. Chem.* **1994**, *33*, 471−476.
(29) Chang, D.; Cocolios, P.; Wu, Y. T.; Kadish, K. M. *Inorg. Chem.* **1984**, *23*, 1629−1633.
(30) Kadish, K. M.; Shao, J.; Ou, Z.; Gros, C. P.; Bolze, F.; Jérôme, F.; Guilard, R. Manuscript in preparation.

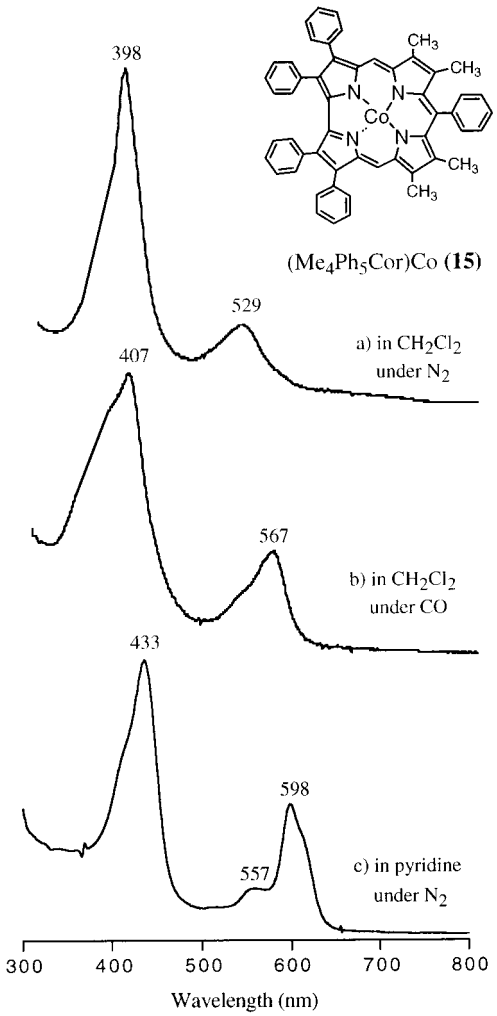

Figure 4. UV−visible spectra of $(Me_4Ph_5Cor)Co$ (**15**) in N_2 or CO saturated CH_2Cl_2 and in N_2 saturated pyridine.

visible band located close to 600 nm for all of the compounds containing phenyl substituents at the corrole macrocycle. These two sets of spectral changes are associated with the stepwise binding of a pyridine molecule to the cobalt ion as shown in eqs 2 and 3 for the case of compound **15**, $(Me_4Ph_5Cor)Co$, whose UV−visible spectra in CH_2Cl_2 and neat pyridine under N_2 are illustrated in Figure 4a,c.

$$(Me_4Ph_5Cor)Co + py \rightleftharpoons (Me_4Ph_5Cor)Co(py) \quad (2)$$

$$(Me_4Ph_5Cor)Co(py) + py \rightleftharpoons (Me_4Ph_5Cor)Co(py)_2 \quad (3)$$

The spectral changes associated with the conversion of $(Me_4Ph_5Cor)Co$, **15,** to its *mono*-pyridine form are shown in Figure 5a and when analyzed by a Hill plot of $\log((A_i - A_0)/(A_f - A_i))$ vs log [py] give a slope of 1.1, consistent with the binding of one pyridine molecule as shown in eq 2. A more substantial change in the UV−visible spectra is seen in Figure 5b, where the Hill plot has a slope of 1.0, consistent with the binding of a second pyridine molecule to $(Me_4Ph_5Cor)Co(py)$, thus generating $(Me_4Ph_5Cor)Co(py)_2$ as shown in eq 3.

It is important to point out that none of the investigated five-coordinate Co(III) complexes show major absorption bands between 550 and 800 nm while the six-coordinate Co(III) species are in each case characterized by an intense absorption band at 593−598 nm for compounds **14**−**18** in pyridine under N_2 and at $\lambda_{max} = 576$ nm for compound **13** which contains only

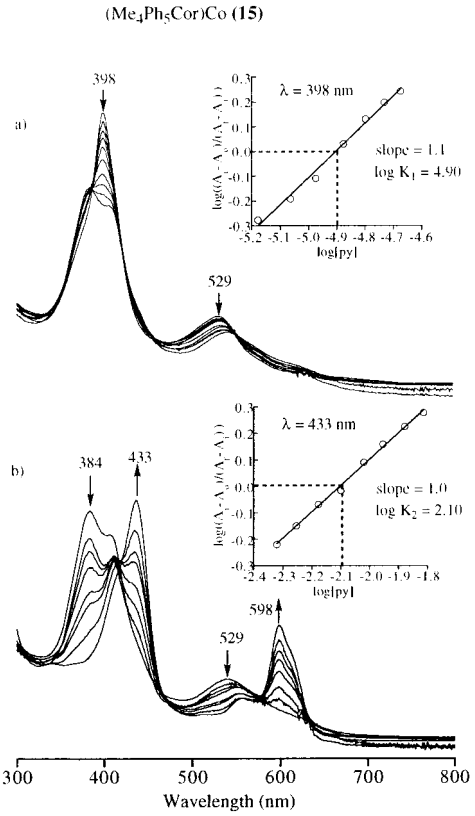

Figure 5. UV−visible spectral changes of 5.0×10^{-6} M $(Me_4Ph_5Cor)Co$ (**15**) during a titration by pyridine in CH_2Cl_2 to give (a) $(Me_4Ph_5Cor)Co(py)$ and (b) $(Me_4Ph_5Cor)Co(py)_2$. The pyridine concentrations for the plots range (a) from 8.7×10^{-6} to 2.1×10^{-5} M and (b) from 4.8×10^{-3} to 1.5×10^{-2} M.

Table 6. Equilibrium Constants of Cobalt Corroles Binding Pyridine or CO in CH_2Cl_2 at 296 K

	pyridine		CO		
compound	log K_1	log K_2	$P_{1/2}^{CO}$ (Torr)	log K[b]	ν_{CO} (cm^{-1})
$(Me_6Et_2Cor)Co$ (**13**)	3.78	2.00	25.3	3.7	2040
$(Et_8Cor)Co$[a]	4.23	1.58			
$(Me_4Ph_5Cor)Co$ (**15**)	4.90	2.10	7.1	4.2	2049
$(Me_4Ph(p\text{-}OMePh)_4Cor)Co$ (**17**)	4.95	2.17	6.4	4.3	2045
$(Me_2Et_2Ph_4Cor)Co$ (**14**)	5.01	2.19	13.0	3.9	2050
$(Me_4Ph(m\text{-}OMePh)_4Cor)Co$ (**16**)	5.32	2.38	5.2	4.3	2049
$(Me_2Ph_7Cor)Co$ (**18**)	5.48	2.19	1.9	4.8	2050

[a] Data were taken from reference 31. [b] $[CO] = k_H \cdot P_{CO}$, $k_H = 6.7 \times 10^{-3}$ M/atm in CH_2Cl_2, and $K = (P_{1/2} \cdot k_H)^{-1}$.

alkyl substituents (see summary of spectral data in Table 5). This intense visible band at close to 600 nm can thus be used as one diagnostic criterium for the occurrence of a bis-pyridine adduct for the neutral complex.

Pyridine binding constants were obtained for each Co(III) corrole, and a summary of the thermodynamic data is given in Table 6. The values of log K_1 range from 3.78 to 5.48, while log K_2 ranges from 2.00 to 2.38. Pyridine binding constants of a similar magnitude were previously measured for the stepwise conversion of $(Et_8Cor)Co$ to $(Et_8Cor)Co(py)$ and then to $(Et_8Cor)Co(py)_2$ in acetone.[31]

The log K_2 values of 2.00−2.38 for compounds **13**−**18** are also close to the values obtained for addition of a single pyridine ligand to $(Me_8Cor)Co(PPh_3)$ (log $K = 2.29$),[3] and these values

(31) Murakami, Y.; Yamada, S.; Matsuda, Y.; Sakata, K. *Bull. Chem. Soc. Jpn* **1978**, *51*, 123−129.

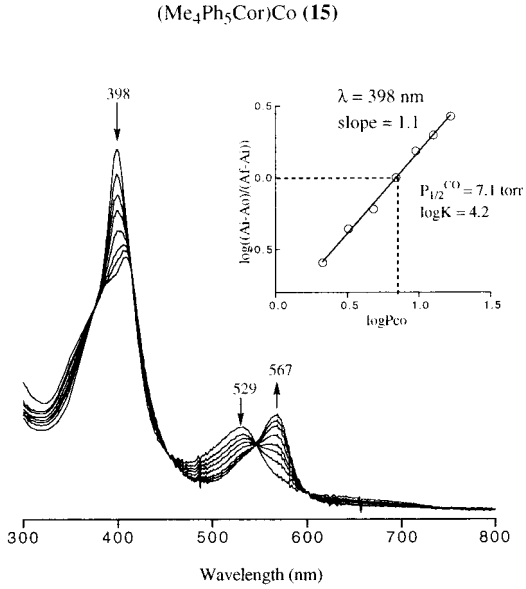

Figure 6. UV−visible spectral changes of 6.0×10^{-6} M (Me_4Ph_5-Cor)Co (**15**) during a titration by CO in CH_2Cl_2. The CO partial pressure ranges from 1 to 230 Torr for the Hill plot.

are slightly higher than the measured log $K = 1.54$ for pyridine addition to (Me_8Ph_3Cor)Co(PPh_3) or to a variety of ($Me_8(XPh)_3$-Cor)Co(PPh_3) complexes, where log K ranges from 1.3 to 1.72 for compounds with X = *p*-OMe, *p*-Me, *p*-Cl, *m*-Cl, or *o*-Cl.[3]

Carbon Monoxide Binding and Electrochemistry under a CO Atmosphere. It is now well-known that Co(III) porphyrins can axially coordinate one or two CO molecules depending upon the nature of the solvent and supporting electrolyte,[32−35] but little is known about the reaction of the cobalt(III) corroles with carbon monoxide. Each cobalt(III) corrole was therefore investigated as to its CO binding ability in CH_2Cl_2.

The UV−visible spectra of the neutral Co(III) corroles were measured under N_2 and under CO. Table 5 compares these spectral data for the cobalt(III) complexes, while Figure 4b shows the spectrum of compound **15** under a CO atmosphere. The spectra were also measured under a variety of CO partial pressures and indicated the binding of one and only one CO molecule to the neutral Co(III) corrole at all CO pressures up to 1 atm. An example of the spectral changes seen upon increasing the CO partial pressure from log $P_{CO} = 0.25$ to 1.25 is shown in Figure 6 for the case of (Me_4Ph_5Cor)Co (**15**), where the initial corrole has absorption maxima at 398 and 529 nm and the *mono*-CO adduct has bands at 407 and 567 nm (see also Figure 4). Well-defined isobestic points are obtained at 369, 450, 546, and 600 nm in the conversion of (Me_4Ph_5Cor)Co to (Me_4Ph_5Cor)Co(CO). The Hill plot of log($(A_i - A_0)/(A_f - A_i)$) vs log P_{CO} (inset of Figure 6) gives a slope of 1.1, thus indicating the binding of one CO molecule to (Me_4Ph_5Cor)Co. The calculated log K for this reaction is 4.2 ($P_{1/2}^{CO} = 7.1$ Torr).

Similar spectral changes were obtained for each of the other corroles as a function of CO partial pressure, and a summary of the binding constants, which range between log $K = 3.7$ and log $K = 4.8$, are given in Table 6 along with the values of ν_{CO} which range from 2040 to 2050 cm^{-1}, depending upon the specific corrole macrocycle. As in the case of py binding, larger log K values are obtained for the five corroles having both aryl and alkyl susbtituents rather than only alkyl substitution (see Table 6).

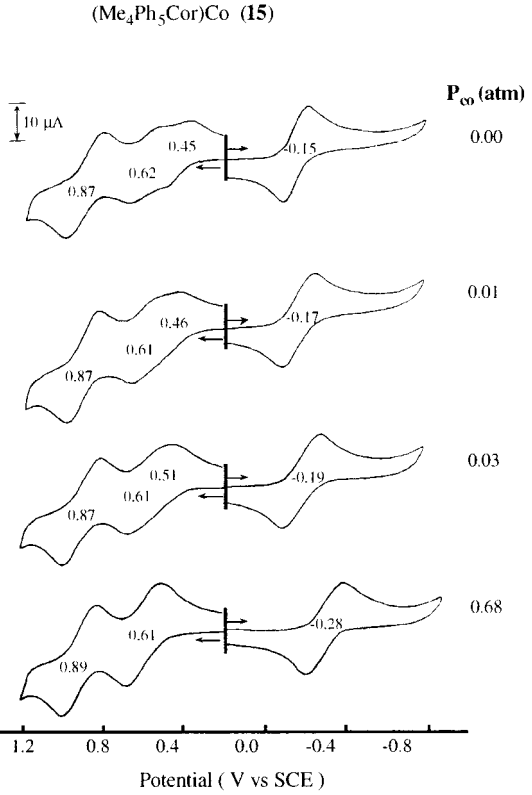

Figure 7. Cyclic voltammogramms of 2.0×10^{-3} M (Me_4Ph_5Cor)Co (**15**) under different CO partial pressures in CH_2Cl_2, 0.1 M TBAP.

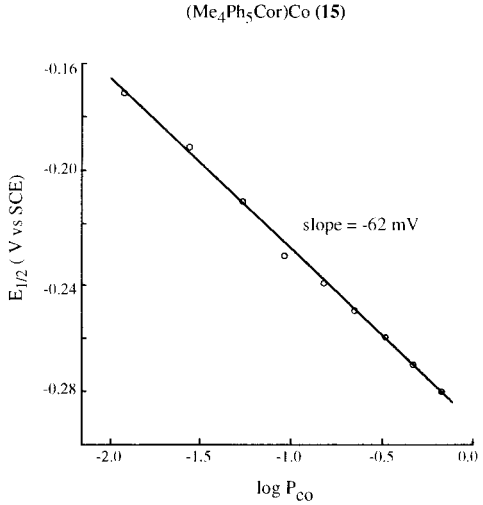

Figure 8. Plot of $E_{1/2}$ for the first reduction of (Me_4Ph_5Cor)Co (**15**) in CH_2Cl_2, 0.1 M TBAP, vs the CO partial pressure (log P_{CO}).

The number of CO molecules bound to compound **15** in CH_2Cl_2 under CO was also monitored by electrochemical methods which plot $E_{1/2}$ vs the CO partial pressure, and an example of the current voltage curves at different CO partial pressure is shown in Figure 7. A plot of $E_{1/2}$ for the first reduction of the compound vs log P_{CO} is linear with a slope of −62 mV shift per each 10-fold increase in CO partial pressure (see Figure 8), and this result can be compared to a theoretical slope of −59 mV per log P_{CO} for the case where one CO molecule binds to the neutral Co(III) corrole but dissociates after

(32) Herlinger, A. W.; Brown, T. L. *J. Am. Chem. Soc.* **1971**, *93*, 1790−1791.
(33) Mu, X. H.; Kadish, K. M. *Inorg. Chem.* **1989**, *28*, 3743−3747.
(34) Hu, Y.; Han, B. C.; Bao, L. Y.; Mu, X. H.; Kadish, K. M. *Inorg. Chem.* **1991**, *30*, 2444−2446.
(35) Schmidt, E.; Zhang, H.; Chang, C. K.; Babcock, G. T.; Oertling, W. A. *J. Am. Chem. Soc.* **1996**, *118*, 2954−2961.

a reversible one-electron reduction to give the Co(II) form of the complex.

This dissociation of CO from the cobalt corrole after electroreduction was verified by thin-layer IR spectroelectrochemistry. An IR band for CO bound to the Co(III) corrole is seen at 2049 cm^{-1} before reduction, and this band disappears after the formation of $[(Me_4Ph_5Cor)Co]^-$ under CO. Under these conditions, the electroreduction is proposed to proceed as shown in eq 4:

$$[(Me_4Ph_5Cor)Co^{III}(CO)] + e \rightleftharpoons [(Me_4Ph_5Cor)Co^{II}]^- + CO \quad (4)$$

Plots of $E_{1/2}$ vs CO partial pressure (Figure 8) also enable a calculation of the CO binding constant for the neutral compound,[33] and in the case of $(Me_4Ph_5Cor)Co(CO)$ the calculated $\log K = 4.4$ is comparable with the $\log K = 4.2$ for CO binding to the same compound determined using UV−visible spectroscopic techniques (see Table 6).

Figure 7 also shows that the first oxidation peak of compound **15** shifts in a positive direction with increasing CO partial pressure, while the second and third oxidations remain virtually unchanged in potential upon going from an N_2 to a CO atmosphere above the solution. The first reversible oxidation of each corrole is associated with formation of the partially oxidized dimer under a nitrogen atmosphere. With an increase of CO partial pressure from 0.00 to 0.68 atm, the first oxidation shifts anodically until it is merged with the second oxidation. When the CO partial pressure is higher than 0.68 atm, only two oxidations, which have the same peak currents as the Co(III)/Co(II) reaction, can be observed.

Similar CO and pyridine binding reactions are seen for compound **15** and for the anthracenyl and biphenylenyl linked bis-corrole Co(III) complexes having the same macrocycle, and this is described in the following paper.[11]

In summary, six cobalt corroles with different numbers of alkyl and aryl substituents were synthesized and investigated as to their electrochemical and ligand binding properties in nonaqueous media. One of the compounds, $(Me_4Ph_5Cor)Co$ (**15**), was then utilized as a comparison compound to study the reactions of face to face bis-corroles whose properties are reported in the following paper in this issue.

Acknowledgment. The support of the Robert A. Welch Foundation (K.M.K., Grant E-680) and the CNRS (Grant UMR 5633) are gratefully acknowledged. The "Région Bourgogne" and "Air Liquide" are acknowledged for a scholarships (F.J.). The authors are also grateful to M. Soustelle for assistance in the synthesis of pyrrole precursors.

Supporting Information Available: Tables of atomic coordinates and their equivalent isotropic thermal parameters and bond distances and angles. This material is available free of charge via the Internet at http://pubs.acs.org.

IC010177+